Rivista Italiana di Paleontologia e Stratigrafia
(*Research in Paleontology and Stratigraphy*)
vol. 130(1): 35-46. **March 2024**
DOI: https://doi.org/10.54103/2039-4942/20461

REWORKED MESOZOIC RADIOLARIANS IN MIOCENE-PLIOCENE FORELAND SEDIMENTS IN THE ZAGROS BELT, IRAN

CHRISTIAN A.F. DIETZEL[1]*, HAYTHAM EL ATFY,[1,2,3] CHRISTOPH BERTHOLD[4], MAHMOUD REZA MAJIDIFARD[5] & MADELAINE BÖHME[1,6]

[1]Terrestrial Palaeoclimatology, Department of Geosciences, Eberhard-Karls-University of Tübingen, Germany.
E-mail: christian.dietzel@uni-tuebingen.de
[2]Palaeobotany Group, Institute for Geology and Palaeontology University of Münster, 48149 Münster, Germany.
[3]Geology Department, Faculty of Science, Mansoura University, 35516 Mansoura, Egypt.
[4]Competence Center Archaeometry – Baden-Wuerttemberg, Eberhard-Karls-University of Tübingen, Germany.
[5]Research Institute for Earth Sciences, Geologic Survey of Iran, Teheran, Iran.
[6]Section Palaeontology, Senckenberg Centre for Human Evolution and Palaeoenvironment, Tübingen, Germany.
*Corresponding author.

Associate Editor: Silvia Gardin.

To cite this article: Dietzel C.A.F., El Atfy H., Berthold C., Reza Majidifard M. & Böhme M. (2024) - Reworked Mesozoic radiolarians in Miocene-Pliocene foreland sediments in the Zagros Belt, Iran. *Riv. It. Paleontol. Strat.*, 130(1): 35-46.

Keywords: Radiolaria; Zagros; sedimentary transport; Cretaceous; Miocene; Pliocene; Iran.

Abstract. Micropaleontology can give important insights into the provenance and paleoenvironmental conditions in terrestrial sedimentary archives. For the current study, 84 samples representing a 2.6 km thick sedimentary profile from the Simply Folded Zagros Mountain Belt were investigated. They span ca. 10.2 my from the late Middle Miocene (Serravallian) to the earliest Pleistocene (Gelasian), and comprise floodplain sediments and saline mudstones with an aeolian contribution. The samples revealed a unique Cretaceous radiolarian assemblage comprising largely of cryptothoracic nassellarians and spherical spumellarians. This record highlights the reworking of sediments derived from Cretaceous Qulqula-Kermanshah radiolarian claystones and radiolarites in the Imbricated Zagros Belt into distal Neogene Zagros foreland sediments in Lurestan (Lurestan Arc). The high abundance of *Holocryptocanium barbui* (Dumitrica) and other cryptothoracic taxa compared to the Qulqula-Kermanshah radiolarian claystones and radiolarites potentially indicates a preferred erosion of softer units such as the Red Radiolarian Claystone Unit (RRCU) compared to harder radiolarian cherts. The observation of a reworked largely cryptothoracic assemblage might also point to additional sorting effects during fluvial and aeolian transport as well as during redeposition, depending on the morphology and hydrodynamic properties of individual radiolarian taxa.

Introduction

In previous paleoclimatic studies, a 2.800 m thick sedimentary succession of Miocene-Pliocene foreland sediments in the Zagros Mountain Belt (Iran) was investigated by soluble salt geochemistry (Böhme et al. 2021) and clay mineralogical analysis (Dietzel et al. 2023). Within the studied profile, the oldest sample (12.6 Ma, Serravallian) taken from the Gachsaran Formation was of coastal-marine origin. In contrast, samples from the lower Aghajari Member (12.02–5.6 Ma, Serravallian-Messinian) show a

Received: June 26, 2023; accepted: February 06, 2024

fluvial-alluvial origin. On top of the studied succession, samples from the Lahbari Member (5.59–2.5 Ma, Messinian-Gelasian) were derived from both aeolian and fluvial-alluvial provenance where soluble salt geochemistry and palynological observations point to a period of sustained hyper-arid climate between 5.6 and 3.3 Ma. This phenomenon was described as the Neogene Arabian Desert climax (NADX), the onset contemporaneous with the acme of the Messinian Salinity Crisis (Böhme et al. 2021). Clay mineralogical investigations throughout the profile (Dietzel et al. 2023) revealed prominent occurrences of autochthonous charophytes in several samples, which were visible even with the naked eye within the sand fraction (> 63 μm), next to few radiolarians. These findings instigated a detailed micropaleontological investigation of all samples to check for further microfossils which could have reliable implications for paleoclimate interpretations as well as sediment provenance. For this purpose, a detailed investigation of the sand fraction in all remaining samples was carried out. The investigation revealed the widespread occurrence of a unique allochthonous Cretaceous radiolarian assemblage throughout the whole sedimentary profile. This reworked radiolarian record closes a gap in understanding the Neogene tectonic obduction of Mesozoic radiolarites in the Zagros mountain belt. Furthermore, it could enhance our knowledge on the effect of erosion and secondary transport on microfossil assemblages such as radiolarians. Henceforth, the current study ultimately aims to detect erosional and transport sorting effects on a reworked radiolarian assemblage and highlight its environmental and ecological impact through time and space throughout the studied material.

Geological overview

The SE–NW trending Zagros Fold and Thrust Belt (ZFTB) resulted from the collision between the Arabian and the Eurasian plates. This collision led to crustal shortening and accommodation of thick sedimentary cover. Deformation intensity is decreasing from the Zagros Suture Zone to the present deformation front, located near the Iran-Iraq border (Alavi 1994; Berberian 1995). The ZFTB belt is tectonically divided, from the SW to the NE, into four zones; (1) the Mesopotamian Foreland Basin with buried folds, extending into the Persian Gulf, (2) the Folded Belt characterized by simple folds, (3) the Imbricated Zone characterized by thrusting, including ophiolite sequences with radiolarites of Jurassic to Cretaceous age (Gharib & De Wever 2010; Al-Qayim et al. 2018); and (4) the Sanandaj–Sirjan metamorphic and magmatic zone (Homke et al. 2004; 2010). The Zagros foreland sediments were, next to an aeolian contribution (Böhme et al. 2021), largely deposited by axial and radial fluvial systems in the Miocene and alluvial fan systems in the Pliocene, derived from the Zagros mountain belt (Koshnaw et al. 2020). Systematic clast analysis revealed the presence of radiolarian chert likely to be derived from erosion of deep marine Qulqula – Kermanshah radiolarites into the Neogene Zagros foreland basin. These clastic sediments have been reported from the proximal conglomerates at the Kirkuk Embayment NNE of the study area (Koshnaw et al. 2017) as well as from the Dezful Embayment towards SE (Etemad-Saeed et al. 2020) and have also been documented in channel-lags from a restricted interval of the Lower Aghajari Member (see below) in the present study area (Böhme et al. 2021) (Fig. 1). However, these clasts have not been comprehensively investigated and there is only limited information on the contribution of radiolarites to other stratigraphic levels as well as to the more distal foreland available sediments, where a finer grain size hampers clast analysis.

The study area near the Iran-Iraq border is part of the Lurestan Arc in the Simply Folded Zagros Belt where syndepositional deformation of foreland sediments has initiated in the Tortonian, possibly between 8.1 and 7.2 Ma (Homke et al. 2004). The investigated mudstone samples cover the Gachsaran Formation, Lower Aghajari Member, Lahbari Member and Bakhtyari Formation. The continuous profiles with a thickness of nearly 2.6 km were sampled in two localities including the Zarrinabad and Changuleh syncline-anticline structures (Fig. 1). The studied samples have robust temporal control, as they were taken at georeferenced sampling points that have been previously dated using magnetostratigraphy by Homke et al. (2004). The sampling points were resampled by Böhme et al. (2021) and are interpolated with numerical age data along the stratigraphic profile. While the clastic rocks from the Zarrinabad profile

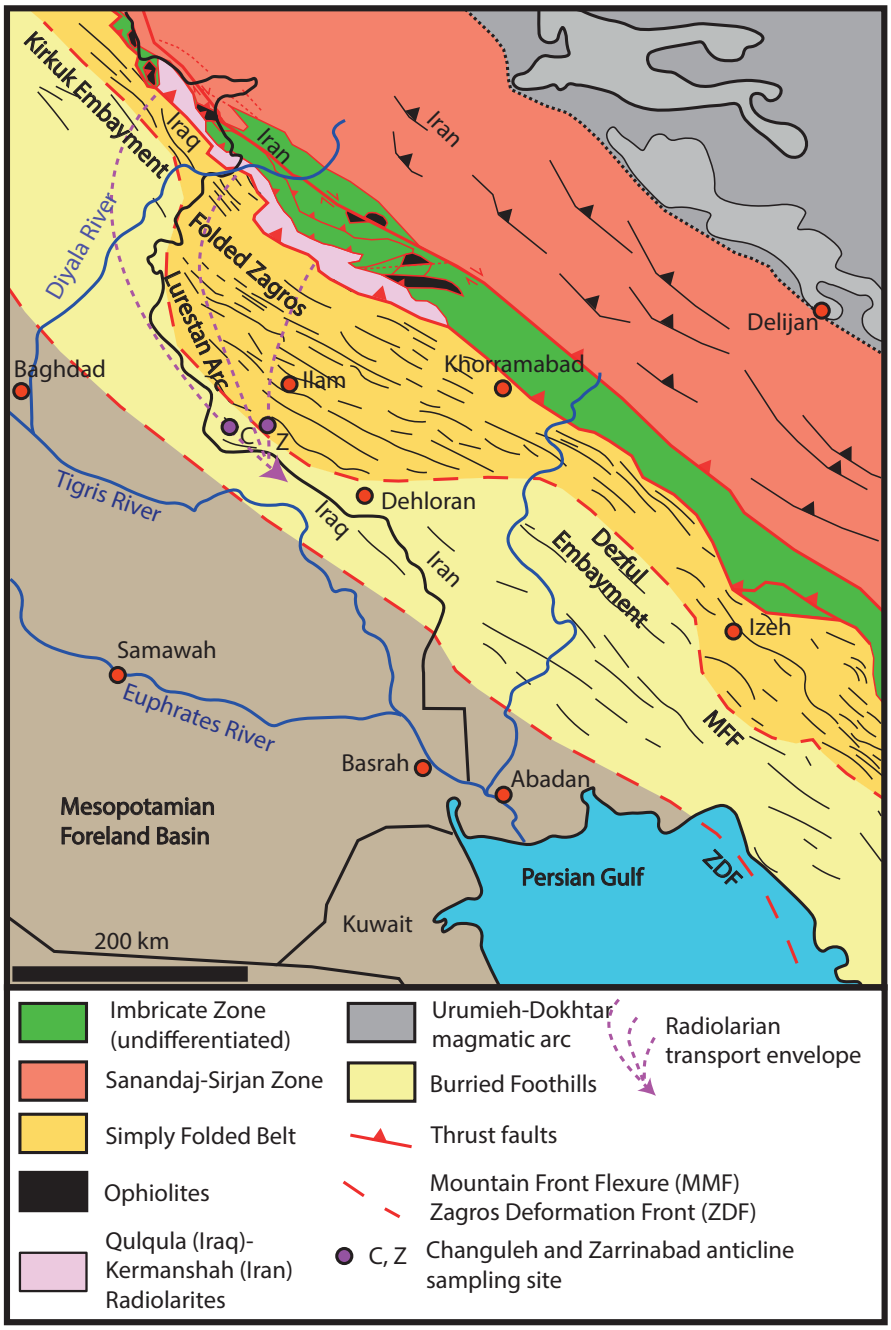

Fig. 1- Structural overview map of the northeastern Mesopotamian Foreland basin. Regional geotectonic map modified from Vergés et al. (2011) with distribution of radiolarites in the Iran-Iraq border region adapted from Ali et al. (2014).

are of late Serrvallian-early Tortonian age (12.6–9.38 Ma), samples from the Changuleh profile are of mid-Tortonian to Pleistocene age (9.02–2.4 Ma). A brief summary of the geological description of the sedimentary profile in (Böhme et al. 2021) is presented here:

In the study area, the upper part of the **Gachsaran Formation** is characterized by alternating reddish mudstones rich in pedogenic gypsum and sandstones with wave ripples, typical of a depositional environment alternating between shallow marine shoreface and terrestrial backshore facies.

The **Aghajari Formation** is divided into the Lower Aghajari Member and the Lahbari Member. The Lower Aghajari Member (12.02–5.6 Ma; Serravallian - Messinian) represents roughly 1.5 km thickness of the sedimentary profile. It is composed of fine-clastic mudstones alternating with and thick fluvial sandstone deposits often showing cross-bedding structures. Channel-lags, between stratigraphic meter 520-770 (10.8 to 9.8 Ma), contain pebble-sized radiolarite-cherts (Fig. 2), which have been not observed in both older or younger horizons. In the Lower Aghajari Member, pedogenic features such

as rhizocretes from carbonate and gypsum as well as manganese staining are commonly observed. Fluvial sandstone channels often feature mud ball erosion at their base. Previous paleoclimate analysis indicates arid conditions during the Serravallian and early Tortonian, followed by semi-arid conditions during the late Tortonian (Böhme et al. 2021; Dietzel et al. 2023), based on soluble salt geochemistry and clay mineralogy. A transition to sustained arid conditions is suggested during the early Messinian. While the sedimentary environment of this rock unit in Khuzestan and Lurestan is characterized by river and lake sedimentation, it represents a coastal-marine facies in Fars.

The **Lahbari Member** (5.59–2.4 Ma; Messinian-lower Gelasian) in the Changuleh anticline is characterized by saline mudstones lacking the pedogenic features observed in the Lower Aghajari Member. Fluvial sandstones are less frequent and generally much thinner than in the underlying member Sediment found in the fine grained Lahbari Member were possibly redeposited locally from the Gachsaran and Aghajari Sediments, which were regionally uplifted in the Lurestan Arc (Emami et al. 2010). The occurrence of structureless, thick silts together with the geochemistry of soluble salts has furthermore been interpreted to indicate an increased aeolian sediment deposition during a hyper-arid period between 5.59 and 3.3 Ma (NADX) (Böhme et al. 2021). Coarse grained alluvial conglomerates can be observed in the upper Lahbari Mb. signifying the progression of the Zagros Mountain Front Flexure near the transition to the conglomeratic Bakhtyari Formation around 2.5 Ma (Homke et al. 2004).

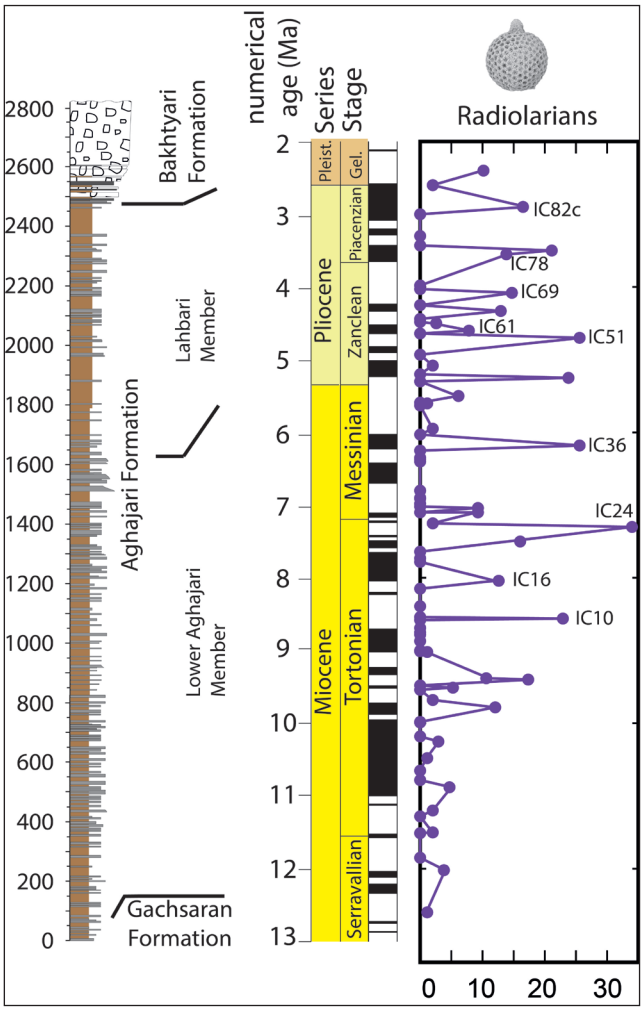

Fig. 2 - Combined stratigraphic profile of the sampling sites at the Zarrinabad anticline and Changuleh syncline-anticline structure. Sedimentary profile and magnetostratigraphic timescale adapted from Homke et al. (2004), sampling points adapted from Böhme et al. (2021). Lines and points represent the numbers of radiolarians found under the binocular in 5g of sediment sample. Number marks sample ID and position of illustrated radiolaria within the profile.

Material and methods

A few kilometres N from the Iran-Iraq border in the Ilam province, Iran, a number of 84 evenly distributed mudstone samples were collected from silty horizons along the 2600 m thick sedimentary profile. Sediments from 12.6 to 9.38 Ma were sampled at the Zarrinabad anticline and from 9.02 to 2.4 Ma at the Changuleh syncline-anticline structure (Fig. 1). As the same samples were previously investigated for paleoclimate analysis, the age model and sample number is identical to Böhme et al. (2021). For the purpose of the current investigation, 5 grams of each sample were dried overnight at 110 °C and then gently disaggregated by hydrating the samples with de-ionized water, utilizing the swelling properties of clay minerals. The samples were then treated with ultrasound for 30 s, to achieve complete separation of clay, silt and sand. The sand fraction was then separated from silt and clay by rinsing the sample through a 63 µm sieve for further micropaleontological investigation (Dietzel et al. 2023). The cleaned samples of the sand fraction were then analysed using a 80 x magnification LEICA S8AP0 binocular. Radiolarians were identified and picked from the sand fraction in 36 samples using a fine brush. 15 selected samples spanning the whole sedimentary profile were then transferred onto a carbon coated sample mount and analysed by a Phenom XL C2 Desktop SEM with 15 kV acceleration voltage.

Results

Thirty-six samples collected throughout the sedimentary profile yielded in total 359 radiolarian specimens (Tab. 1 supplement, Fig. 2). A general increase of radiolarians per productive sample is observed after ~10 Ma. The retrieved radiolarians were found in sediment samples from the Gachsaran Formation, Lower Aghajari Member and Lahba-

ri Member. Their size varied from 90–360 μm and comprised Nassellaria with a large spherical abdomen and Spumellarians. The majority of all recognizable skeletons showed hexagonal surface ornamentations. Specific identification to a species level was only possible for few specimens due to surface damage, recrystallization and abrasion likely related to secondary transport. This is aggravated by the general similarities of the surface morphology of Nassellarian taxa such as, *Cryptamphorella* sp. or *Holocryptocanium barbui* (Dumitrica) (Pl. 2). Furthermore, identification was hampered by the fact, that the allochthonous nature of the radiolarians did not allow for age cross-referencing between individual radiolarians in one individual sample. Their lowest and highest occurrence ranges were compiled after previous works. The known stratigraphic range of specifically identified radiolarians was plotted next to the age span of the Kermanshah-Qulqula radiolarites as a possible source (Gharib & De Wever 2010; Al-Qayim et al. 2018) (Fig. 3). Furthermore, the presence of other marine taxa represented by foraminifera was noted in sample IC10 (8.56 Ma) and in IZ157 (9.54 Ma), IC69 (4.08 Ma) and IC 82c (2.9 Ma), that are beyond the scope of this investigation.

Systematic paleontology

Class RADIOLARIA Müller, 1858
Subclass POLYCYSTINEA Ehrenberg, 1839, emend. Riedel, 1967
Order **Nassellaria** Ehrenberg, 1875
Family Archaeodictyomitridae Pessagno, 1976
Genus *Tharnala* Pessagno, 1977

Tharnala sp.
Plate 1, fig. a

Occurrence: sample IC21 7.5 Ma.

Family Artostrobiidae Riedel, 1967
Genus *Rhopalosyringium* Campbell & Clark, 1944

Rhopalosyringium sp.
Plate 1, fig. b

Occurrence: sample IC69, 4.08 Ma.

Family Williriedellidae Dumitrica, 1970
Genus *Cryptamphorella* Dumitrica, 1970

Cryptamphorella conara Foreman, 1968
Plate 1, fig. c

Occurrence: sample IC51, 4.7 Ma.
Stratigraphic range of the taxon: Albian-Maastrichtian (Bandini et al. 2008).

Cryptamphorella sp. cf. ***C. conara*** Foreman, 1968
Plate 1, fig. d; Plate 2, fig. h

Occurence: sample, IC21, 7.5 Ma; IC51 4.7 Ma.

Cryptamphorella**?** sp.
Plate 1, fig. e

Occurrence: sample IC82c, 2**.**9 Ma.

Genus *Holocryptocanium* Dumitrica, 1970

Holocryptocanium barbui Dumitrica, 1970
Plate1, fig. f; Plate 2, figs. a-c, f

Occurrence: samples IC36 6.18 Ma; IC 51, 4.7 Ma; IC61, 4.6 Ma.
Stratigraphic range of the taxon: Tithonian-Turonian (Bragina & Bragin 2021; Baumgartner et al. 2023).

Holocryptocanium sp. cf. ***H. astiense*** Pessagno, 1977
Plate 1, fig. g

Occurrence: sample IC 61, 4.6 Ma.
Stratigraphic range of the taxon: Cenomanian-Coniacian (Bragina & Bragin 2021).

Order **Spumellaria** Ehrenberg, 1875
Family Dactyliosphaeridae Squinabol, 1904
Genus *Dactyliosphaera* Squinabol 1904

Dactyliosphaera**?** sp.
Plate 1, fig. h

Occurrence: sample IC10, 8.56 Ma.

Family Parvivaccidae Pessagno & Yang, 1989, emend. Dumitrica & Caulet, in De Wever et al. (2001)
Genus *Praeconosphaera* Yang, 1993

Praeconosphaera sp. cf. ***P. antiqua*****?** Parona, 1890
Plate 1, fig. i

Occurrence: samples IC16, 8.04 Ma; IC51, 7.7 Ma; IC78, 3.55 Ma.
Remarks. Possibly a cryptocehalic nasselarian.

Family Praeconocaryommidae Pessagno, 1976

Genus *Praeconocaryomma* Pessagno, 1976

Praeconocaryomma sp. cf. ***P californiensis*** Pessagno, 1976

Plate 1, fig. j

Occurrence: sample IC10, 8.56 Ma; sample IC 24, 7.3 Ma.
Stratigraphic range of the taxon: Upper Cenomanian-Campanian (Bragina 2004).

Family Xiphostylidae Haeckel, 1881
Genus *Archaeocenosphaera* Pessagno, 1989

***Archaeocenosphaera*?** sp.

Plate 1, fig. k; Plate 2, fig. i

Occurrence: sample IC26, 7.04 Ma, IC21, 7.5 Ma.

Archaeocenosphaera clathrata Parona, 1890

Plate 1, fig. l

Occurrence: IC78, 3.55 Ma.
Stratigraphic range of the taxon: Lower Devonian-Eocene (Ozsvárt et al. 2020).

Archaeocenosphaera*? *mellifera O'Dogherty, 1994

Plate 1, fig. m

Occurrence: sample IC16, 8.04 Ma.
Stratigraphic range of the taxon: Albian-Campanian (Bragina et al. 2022).

Gen. et spec. indet. 1

Plate 1, fig. n

Occurrence: sample IC 21 at 7.5 Ma.
Remarks. This taxon describes a spherical internal mold of a radiolarian skeleton.

Gen. et spec. indet. 2

Plate 1, fig. o

Occurrence: sample IC61, 4.6 Ma.
Remarks. This taxon describes a spherical mould of 80 µm diameter and displays protruding imprints of pore structure.

Gen. et spec. indet. 3

Plate 2, fig. d

Occurrence: sample IC36 6.18 Ma.

Gen. et spec. indet. 4

Plate 2, fig. e

Occurrence: sample IC36 6.18 Ma.

Gen. et spec. indet. 5

Plate 2, fig. g

Occurrence: sample IC36 6.18 Ma.

Discussion

Sediment provenance and tectonic implications

Regarding mineralogical composition, the sediments of the Aghajari Member are mostly composed of quartz, feldspar, volcanic, and metamorphic lithoclasts sourced from Eurasia. The composition of detrital Cr-spinels also indicates a contribution of mafic to ultramafic ophiolites of the Arabia-Eurasia suture zone to the foreland sediments (Cai et al. 2021). The ophiolites of the Zagros suture zone are currently exposed alongside radiolarite nappes in Kermanshah and Neyriz in Iran (Stoecklin 1968; Cai et al. 2021) and can also be found NW along strike in Iraq and Turkey (Jassim & Goff 2006; Ismail et al. 2010). The Zagros radiolarites found within the Imbricate Zagros have been described in the literature as Qulqula radiolarites in Iraq and Kermanshah radiolarites in Iran. They have been micropaleontologically constrained to the lower Pliensbachian up to the Turonian at Kermanshah, Iran (Gharib & De Wever 2010) and Bajocian to the end of the Cenomanian at Qulqula, Iraq (Al-Qayim et al. 2018). Reworked radiolarians identified in this study in the Zagros foreland sediments are generally of Cretaceous age while Jurassic ones are poorly represented. Although the Qulqula – Kermanshah radiolarites of the Arabia-Eurasia suture zone 200-300 km north of the study area (Fig. 1) are indicated as the general source area, the limited presence of reworked Jurassic taxa might be either due to a better preservation potential of Cretaceous taxa or a minor occurrence of Jurassic radiolarites in the direct erosional area. The assumed source area agrees with paleoflow directions in the floodplain sediments and radiolarian claystones of the Aghajari Member in the study area pointing towards SE as the present-day Tigris river (Homke et al. 2004). The presence of radiolarite clasts have been described throughout the Zagros Foreland Basin (Koshnaw et al. 2017; Etemad-Saeed et al. 2020; Böhme et al. 2021). Radiolarians from these clasts

PLATE 1

SEM-Illustrations of allochthonous Jurassic and Cretaceous Radiolaria found in Lower Aghajari Member and Lahbari Member.
a) *Tharnala* sp. sample IC21 7.5 Ma; b) *Rhopalosyringium* sp. sample IC69, 4.08 Ma; c) *Cryptamphorella conara* Foreman, 1968 sample IC51, 4.7 Ma; d) *Cryptamphorella* sp. cf. *C. conara* Foreman, 1968, sample IC21, 7.5 Ma; e) *Cryptamphorella*? sp. 2 sample IC82c, 2.9 Ma; f) *Holocryptocanium barbui* Dumitrica, 1970 sample IC 51, 4.7 Ma; g) *Holocryptocanium* sp. cf. *H. astiense* Pessagno, 1977 sample IC 61, 4.6 Ma; h) *Dactyliosphaera*? sample IC10, 8.56 Ma; i) *Praeconosphaera* sp. cf. *P. antiqua*? Parona, 1890 sample IC51 4.7 Ma; j) *Praeconocaryomma* sp. cf. *C. californiensis* Pessagno, 1976, sample IC 24, 7.3 Ma; k) *Achaeocenosphaera*? sp. sample IC26, 7.04 Ma; l) *Archaeocenosphaera clathrata* Parona, 1890 sample IC78, 3.55 Ma; m) *Archaeocenosphaera*? *mellifera* O'Dogherty 1994 sample IC16, 8.04 Ma; n) Gen. et spec. indet. 1 sample IC 21 7.5 Ma o) Gen. et sp. indet. 2, sample IC61, 4.6 Ma.

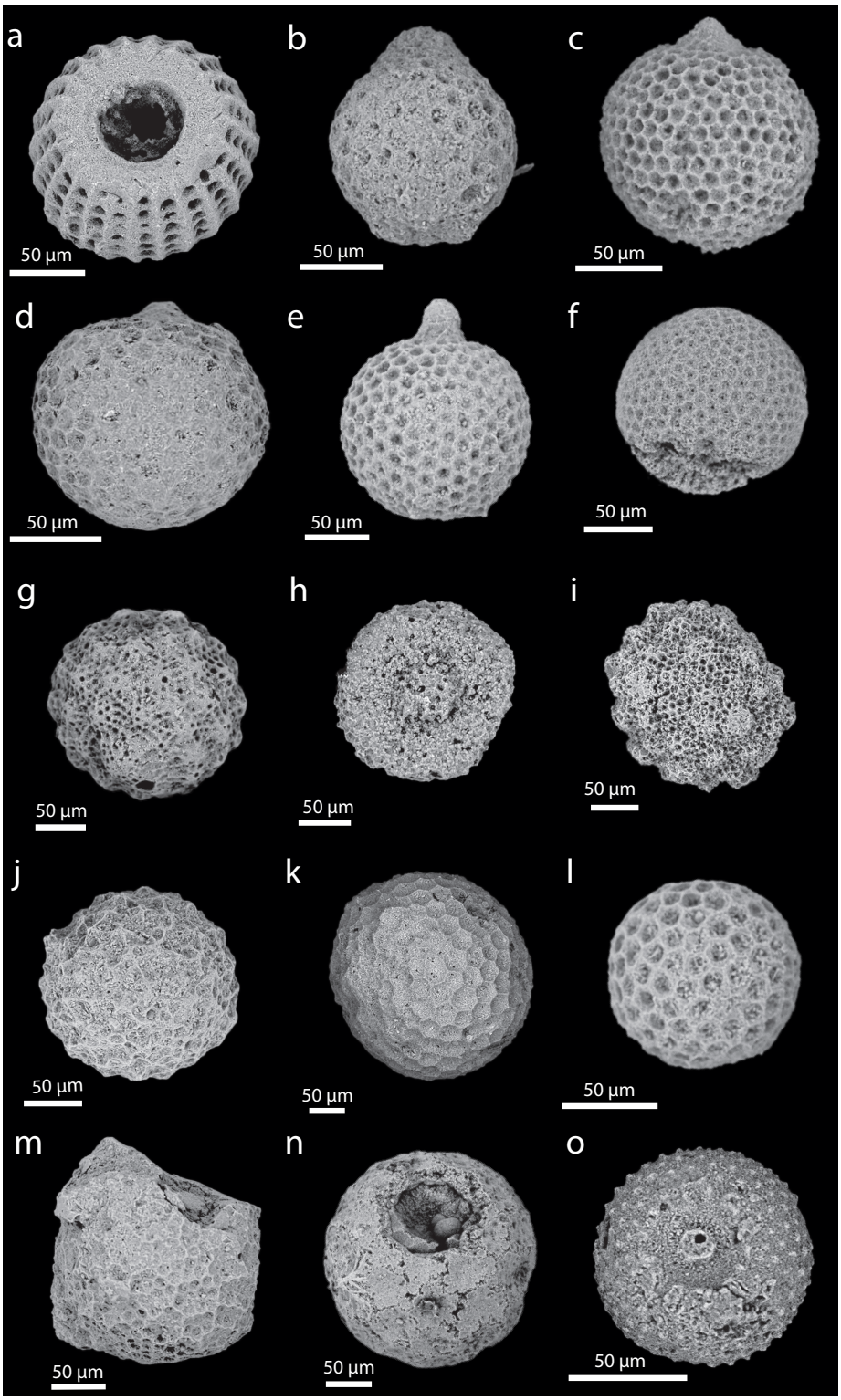

would likely be better suited for age determination due to a higher preservation potential; however, no clasts were available for comparison in this study. An increase in the proportion of radiolarite clasts has been reported in conglomerates from the Zagros foreland sediments in the Dezful embayment, 200 km SE of this study area, in the mid-Tortonian ~ 9 Ma and was linked to tectonic exhumation and erosion of the Kermashah radiolarites in the Imbricated Zagros NE of the Dezful Embayment (Etemad-Saeed et al. 2020). An earlier increase in the radiolarians per sample is observed in the samples of this study at ~ 10 Ma (Fig. 2), possibly indicative of an earlier increased tectonic exposure of

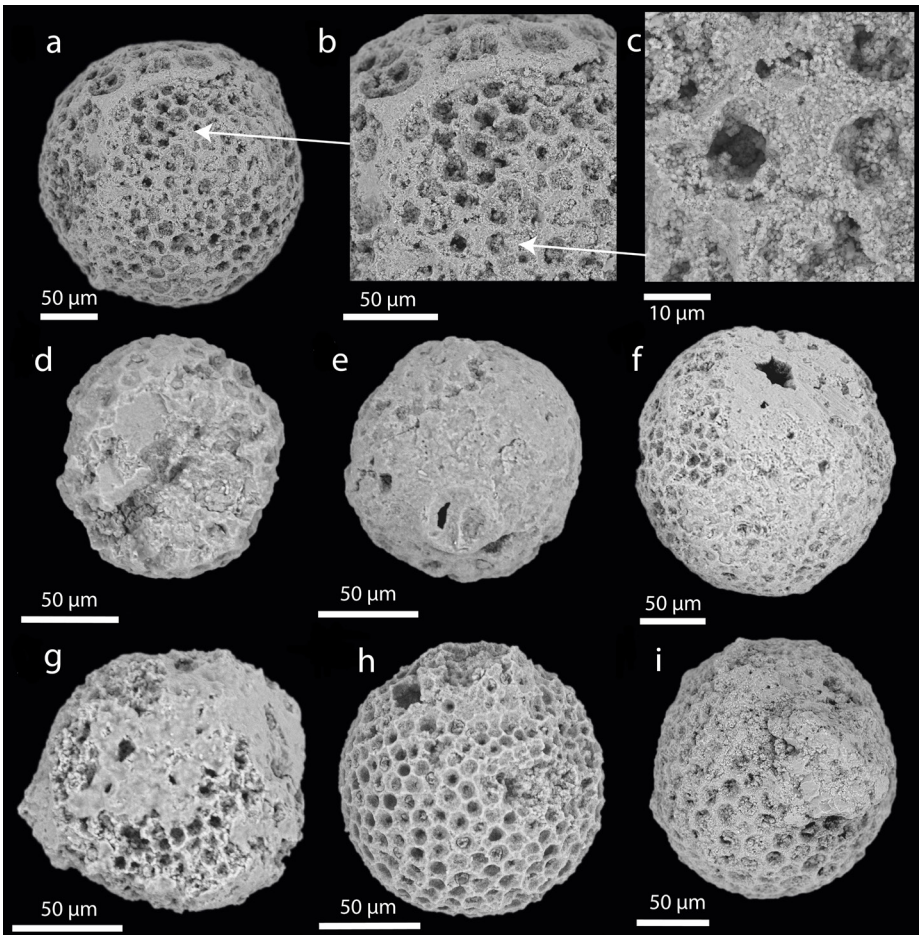

PLATE 2

SEM-Illustrations of typical preservation allochthonous radiolarians with hexagonal pore structure found in Miocene-Pliocene foreland sediments of the Pust-e Kuh arc.

a-c) *Holocryptocanium barbui* Dumitrica, 1970 recrystallization and partial overgrowth of radiolarian skeleton with SiO_2 infill of pore spaces and abdomen with fine grained quartz crystals sample IC61, 4.6 Ma; d) Gen. et sp. indet. 3, complete recrystallization of pore-space with SiO_2 extremely poor preservation of surface, potential transport damage, sample IC36 6.18 Ma; e) Gen. et sp. indet. 4 hollow radiolarian skeleton showing recrystallization of surficial pore space with SiO_2, with abrasion damage on the surface, sample IC36 6.18 Ma; f) *Holocryptocanium barbui* Dumitrica, 1970 hollow skeleton showing recrystallization of surficial pore space and limited infill of the abdomen with SiO_2, some abrasion damage on the surface, sample IC36 6.18 Ma; g) Gen. et sp. indet. 5, a recrystallized skeleton with growth of clay minerals and carbonate, sample IC36 6.18 Ma; h) *Cryptamphorella* sp. cf. *C. conara* Foreman, 1968 abraded cephalo-thoracic portion. partial infill of pores with SiO_2, sample IC51 4.7 Ma.; i) *Archaeocenosphaera*? sp., recrystallized skeleton with fine-grained SiO_2 infill of pore spaces, overgrowth of coarse-grained SiO_2 on the surface, sample IC21 7.5 Ma.

the Qulqula – Kermanshah radiolarites NE of the Lurestan Arc compared to the Dezful embayment.

The presence of allochthonous radiolarians likely derived from Qulqula – Kermanshah radiolarites throughout the uppermost part of the Gachsaran Formation, Lower Aghajari Member, and the Lahbari Member indicates a continuous sediment input originating from the Imbricated Zagros to the North and East of the study area during the Miocene and Pliocene. In the Lahbari Member, between 5.59 and 3.3 Ma, Böhme et al. (2021) suggested enhanced aeolian input from a westerly sediment source based on the heavy mineral spectrum during the hyper-arid NADX phase. In the case of a long-range-aeolian sediment transport from a sediment source in the west, a change in microfossil assemblage would also be expected compared to the fluvial deposits of the Lower Aghajari Member. The sustained observation of radiolarians likely derived from Qulqula – Kermanshah radiolarites is, however, more indicative of a sediment origin to the NNE. Therefore, the presence of radiolarians in the Lahbari Member is better explained by the redeposition of the local Gachsaran and Aghajari sediments regionally uplifted in the Pusht-e Kuh Arc to the North and East of the Changuleh Anticli-

ne, according to the model of Emami et al. (2010). Hereby aeolian processes likely played an important role in regional sediment redeposition leading to the formation of thick, structureless, saline siltstones of the Lahbari Member in front of the Lurestan Arc (cf. Böhme et al. 2021).

Impact of erosion and redeposition on radiolarian assemblages

Erosion

While frequent radiolarian chert clasts were described by Etemad-Saeed et al. (2020), clasts of radiolarite chert were only recognized between 10.8 to 9.8 Ma in the Zarrinabad section of the profile (Böhme et al. 2021). Unfortunately, no sample of these cherts was taken in the field for analysis. Only single radiolarians without major chert attachments were observed throughout the fine-grained sandstones and mudstones of this study. This could correspond to the mobilization of single radiolarians from softer claystones such as the Red Radiolarian Claystone Unit (RRCU). *Holocryptocanium barbui* (Dumitrica) is the most commonly observed taxon in this study. In the Qulqula – Kermanshah radiolarites *H. barbui* (Dumitrica) has so been observed in the RRCU (Al-Qayim et al. 2018), where it has been reported alongside *Archaeodictyomitra mitra* (Dumitrica), *Angulobracchia portmanni* s.l. (Baumgartner) and *Pseudodictyomitra carpatica* (Lozyinak). The radiolarian claystones of the RRCU are of Berriasian to early Aptian age (Al-Qayim et al. 2018). They possibly represent the "Crypto-Archaeo" Assemblage, comprising low diversity, ecologically tolerant forms (chiefly cryptocephalic and cryptothoracic nassellarians and *Archeodictyomitra* spp.) which have been interpreted to originate in the Subtropical Gyre (Baumgartner et al. 2023). Enhanced erosion of radiolarians from these softer low-diversity radiolarian claystones compared to interbedded harder radiolarian cherts or limestones is therefore possibly a prime factor accounting for the high percentage of cryptothoracic nassellarians observed in this study, while other radiolarian taxa described from radiolarites Gharib and De Wever (2010) and Al-Qayim et al. (2018) are missing. The RRCU with a thickness of 80-100 m has only been analysed by a single sediment sample so far (KN-32), therefore the age span covered given by Al-Qayim et al. (2018) might possibly be too short.

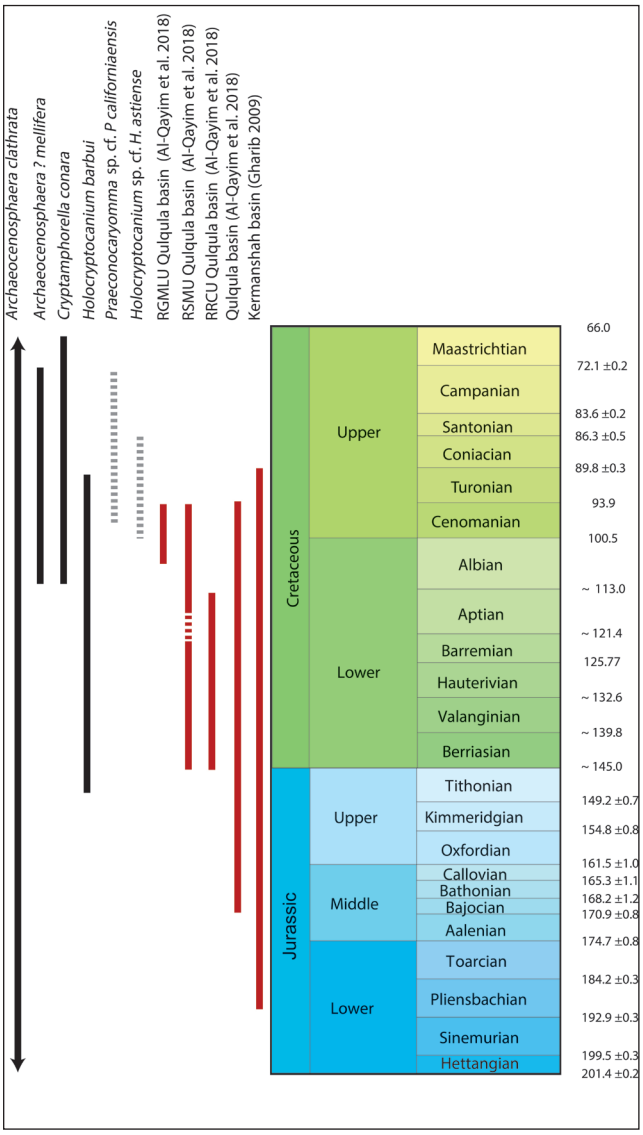

Fig. 3 - Stratigraphic chart marking the total range of occurrence of Mesozoic radiolarian taxa identified in Zagros foreland sediments and the age of radiolarites in the Qulqula – Kermanshah basins as potential source area. Grey dotted bars indicate a higher level of uncertainty in the determination of taxon.

This might explain the missing age range overlap between the RRCU and some of the cryptothoracical taxa observed in this study such as *Cryptamphorella conara* (Foreman) (Fig. 3). A temporal overlap for mid- to Late Cretaceous radiolarian taxa found in this study is found in the Red Siliceous Mudstone Unit (RSMU) of up to 50 m thickness comprising thin to medium bedded radiolarian mudstone and shale alternating with siliceous shale, and minor limestone and chert, as well as the Reddish-Green Mudstone and Limestone Unit (RGMLU) of up to 20 m thickness comprising alternation of red and green marly mudstones and claystones, with thin to

medium beds of calcilutite to calcisiltite bioclastic to peloidal limestone (Al-Qayim et al. 2018). While the RSMU and RRCU have been interpreted to have been deposited the distal abyssal plane, the RGMLU has been interpreted to represent the proximal slope of the Afro-Arabian Margin. A single radiolarian bearing pelagic limestone sample (KN-2) of the middle Albian to Cenomanian RGMLU and a single middle Aptian-Cenomanian radiolarian shale sample (KN-3) of the RSMU were assessed in Al-Qayim et al. (2018). While the described assemblages did contain *Tharnala praeveneta* (Pessagno) and *Tharnala pulchra* (Squinabol) in sample KN-2, they do not match well with the reworked Middle-Upper Cretaceous cryptothoracic Nasselarians observed in this study. No taxonomic data was available on the radiolarian assemblages of the interbedded softer mudstones and claystones found within the RGMLU and RSMU. Further future high-resolution studies in the Qulqula – Kershmanshah radiolarites and radiolarian claystones are therefore warranted.

Transport

Additionally, compact spherical radiolarians could have been enriched during transport. It seems possible that compact spherical taxa show more resistance to breaking during turbulent fluvial erosion and transport than complexly branched taxa with long-producing spines. A turbulent transport history is implied by the evidence of surface abrasion and chipped-off surface structure visible on many radiolarian skeletons (Pl. 2) All radiolarians observed in this study show a varying degree of recrystallization of SiO_2 (Pl. 2). If this infill of diagenetic SiO_2 predates the erosion of the primary radiolarites during the Miocene and Pliocene, it might have further strengthened the structure of the individual radiolarians giving more resistance against erosional processes. An additional model for preferential transport could be provided by the sorting processes of aeolian transport, such as dust storms, which preferentially transport well-rounded silt and sand grains (Mazzullo et al. 1992) along the semi-arid to the hyper-arid flood plain.

Deposition

Furthermore, settling velocities of different radiolarian taxa need to be considered. For this study only mudstones were analyzed, while the interbedded coarser grained sandstones were not tested. It is therefore possible that larger taxa could have been deposited preferentially within the coarser sandstones along the floodplain. The departure of a grain from a spherical shape causes a decrease in its settling velocity within a fluid (Komar & Reimers 1978). Experimental work by Takahashi and Honjo (1983) on extant radiolarian skeletons indicated a variation in sinking speed in seawater between 13 and 416 m per day. The observed sinking speeds are generally lower than those predicted by Stokes Law and systematically deviate from it. In the experimental study the weight per shell showed the highest correlation with sinking speed, while some taxa with a large spine surface demonstrated significantly reduced sinking rates. Compact, spherical taxa filled with recrystallized silica might therefore be expected to settle to the ground quicker in a slowly flowing river, than radiolarians of a more complex structure with a higher surface-weight ratio.

It cannot be ruled out, however, that fragile radiolarians have been damaged further during the sample dispersion process. However, no obvious fragments were found during the picking of radiolarians. Smaller fragments might also have been lost during the sieving process in a 63 μm sieve. The observation of strong sorting of radiolarians contrasts with a report of reworked Upper Cretaceous radiolarians described in the Eocene marine London clay formation, where no such sorting has been observed (Fer et al. 2016). While the authors described a generally poor preservation of radiolarians as also found in this study, the source and mode of transport of these reworked radiolarians was uncertain. Differences could also apply as the radiolarians in this study were deposited within a mudstone of a fluvial environment. In contrast, the assemblage reported by Fer et al. (2016) was deposited in a marine environment.

Conclusion

Cretaceous radiolarians throughout the uppermost part of the Gachsaran Formation, Lower Aghajari Member, and Lahbari Member is a unique record for terrestrial sediments. This indicates a continuous contribution of eroded Mesozoic radiolarites from the tectonically obducted Kermanshah – Qulqua radiolarite complex located in the Imbricated Zagros to the Foreland sediments in the Lu-

restan arc during the Late Miocene and Pliocene, which increased during the Tortonian at ~ 10 Ma. The allochthonous radiolarian assemblage is mainly characterized by several taxa of recrystallized, compact, spherical Nassellarians and Spumellarians. This assemblage is distinct from the autochthonous assemblage reported from the Kermanshah-Qulqula radiolarites as a potential source region and shows some similarities to the assemblage described from the Red Radiolarian Claystone Unit (RRCU) of the Qulqula radiolarites. This observation might suggest a selectively enhanced erosional mobilization of radiolarians from the softer radiolarian claystones compared to harder radiolarites. Furthermore, it seems possible that compact spherical taxa provide more stability during transport than more elongated or branched-shaped radiolarian skeletons. It is also possible that these taxa have a higher Stokes settling velocity in slow-flowing fluvial systems than taxa with a higher surface-to-weight ratio, leading to an increased deposition in fluvial sediments.

Acknowledgements: We would like to thank Tatiana Miranda and Hartmut Schulz for supervision the SEM work and Martin Ebner for his fruitful discussions. It is a pleasure to acknowledge Silvia Spezzaferri for the valuable input regarding the identification of microfossils. We are most grateful to Peter Baumgartner and three anonymous reviewers for their constructive reviews, which greatly improved the manuscript.

References

Al-Qayim B.A., Baziany M.M. & Ameen B.M. (2018) - Mesozoic Tethyan Radiolarite age determination, Zagros suture zone, Kurdistan, NE Iraq. *The Iraqi Geological Journal*: 17-33.

Alavi M. (1994) - Tectonics of the Zagros orogenic belt of Iran: new data and interpretations. *Tectonophysics,* 229(3-4): 211-238, 234.

Ali S.A., Mohajjel M., Aswad K., Ismail S., Buckman S. & Jones B. (2014) - Tectono-stratigraphy and structure of the northwestern Zagros collision zone across the Iraq-Iran border. *Faculty of Science, Medicine and Health - Papers*: part A. 2058.

Bandini A.N., Flores K., Baumgartner P.O., Jackett S.-J. & Denyer P. (2008) - Late Cretaceous and Paleogene radiolaria from the Nicoya Peninsula, Costa Rica: a tectonostratigraphic application. *Stratigraphy,* 5(1): 3-21.

Baumgartner P.O., Li X., Matsuoka A. & Vérard C. (2023) - Austral and Subtropical Gyre Radiolaria-latest Jurassic to Early Cretaceous Leg 123, Site 765, Argo Abyssal Plain revisited: Southern Hemisphere paleobiogeography and global climate change. *Micropaleontology,* 69(6).

Berberian M. (1995) - Master "blind" thrust faults hidden under the Zagros folds: active basement tectonics and surface morphotectonics. *Tectonophysics,* 241(3-4): 193-224, 200.

Böhme M., Spassov N., Majidifard M.R., Gärtner A., Kirscher U., Marks M., Dietzel C., Uhlig G., El Atfy H. & Begun D.R. (2021) - Neogene hyperaridity in Arabia drove the directions of mammalian dispersal between Africa and Eurasia. *Communications Earth & Environment,* 2(1): 1-13.

Bragina L. (2004) - Cenomanian-Turonian radiolarians of northern Turkey and the Crimean Mountains. *Paleontological Journal,* 38: S325-S456.

Bragina L. & Bragin N. (2021) - Radiolaria from the lower Cenomanian (Upper Cretaceous) of Crimea. Part 2. Nassellaria. *Revue de Micropaléontologie,* 71: 100482.

Bragina L., Proshina P., Bragin N., Tsiolakis E., Symeou V. & Papadimitriou N. (2022) - Radiolaria and planktonic foraminifera from Sarama composite section of the Kannaviou Formation (Campanian, Upper Cretaceous, Cyprus). *Palaeoworld,* 31(4): 704-722.

Cai F., Ding L., Wang H., Laskowski, A.K., Zhang L., Zhang B., Mohammadi A., Li J., Song P. & Li Z. (2021) - Configuration and timing of collision between Arabia and Eurasia in the Zagros collision zone, Fars, southern Iran. *Tectonics,* 40(8): 1-21, 18.

Campbell A.S. & Clark B.L. (1944) - Radiolaria from upper Cretaceous of middle California. *Geological Society of America, Special Papers*. 57: 1-61.

De Wever P., Dumitrica P., Caulet J.P., Nigrini C. & Caridroit M. (2001) - Radiolarians in the sedimentary record. CRC Press, 28 feb 2002, 533 pp.

Dietzel C.A., Berthold C., Kirscher U., Majidifard M.R. & Böhme M. (2023) - Using clay mineralogy and micropalaeontological observations to unravel Neogene climate variations in Northern Arabia. *Arabian Journal of Geosciences,* 16(5): 343.

Dumitrica P. (1970) - Cryptocephalic and cryptothoracic Nassellaria in some Mesozoic deposits of Romania. *Revue Roumaine de Géologie Géophysique et Géographie*, 14(1): 45-124.

Ehrenberg C.G. (1875) - Fortsetzung der mikrogeologischen Studien als Gesammt-Ubersicht der mikroskopischen Palaontologie gleichartig analysirter Gebirgsarten der Erde, mit specieller Rucksicht auf Polycystinen-Mergel von Barbados. *Abhandlungen der Koniglichen Akademie der Wissenschaften zu Berlin* 1875 (1875): 1-226.

Emami H., Vergés J., Nalpas T., Gillespie P., Sharp I., Karpuz R., Blanc E. & Goodarzi M. (2010) - Structure of the Mountain Front Flexure along the Anaran anticline in the Pusht-e Kuh Arc (NW Zagros, Iran): insights from sand box models. *Geological Society, London, Special Publications,* 330(1): 155-178, 173.

Etemad-Saeed N., Najafi M. & Vergés J. (2020) - Provenance evolution of Oligocene–Pliocene foreland deposits in the Dezful embayment to constrain Central Zagros exhumation history. *Journal of the Geological Society,* 177(4): 799-817.

Fer T., Danelian T. & Bailey H.W. (2016) - Upper Cretaceous radiolarians reworked in the Eocene London Clay Formation, SE England. *Journal of Micropalaeontology,* 35(2): 133-142.

Foreman H.P. (1968) - Upper Maastrichtian Radiolaria of California. *Special Papers in Palaeontology* 3: 1-82.

Gharib F. & De Wever P. (2010) - Radiolaires mésozoïques de la formation de Kermanshah (Iran). *Comptes Rendus Palevol,* 9(5): 209-219.

Haeckel E. (1881) - Prodromus systematis radiolarium, Entwurf eines Radiolarien-Systems auf Grund von Studien der challenger-radiolarien. *Jenaische Zeitschrift für Naturwissenschaft,* 15: 418.

Homke S., Vergés J., Garcés M., Emami H. & Karpuz R. (2004) - Magnetostratigraphy of Miocene–Pliocene Zagros foreland deposits in the front of the Push-e Kush arc (Lurestan Province, Iran). *Earth and Planetary Science Letters,* 225(3-4): 397-410.

Homke S., Vergés J., Van Der Beek P., Fernandez M., Saura E., Barbero L., Badics B. & Labrin E. (2010) - Insights in the exhumation history of the NW Zagros from bedrock and detrital apatite fission-track analysis: Evidence for a long-lived orogeny. *Basin Research,* 22(5): 659-680, 660.

Ismail S.A., Mirza T.M. & Carr P.F. (2010) - Platinum-group elements geochemistry in podiform chromitites and associated peridotites of the Mawat ophiolite, northeastern Iraq. *Journal of Asian Earth Sciences,* 37(1): 31-41, 33.

Jassim S.Z. & Goff J.C. (2006) - Geology of Iraq. DOLIN, s.r.o., distributed by Geological Society of London, 2006, 341 pp.

Komar P.D. & Reimers C. (1978) - Grain shape effects on settling rates. *The Journal of Geology,* 86(2): 193-209.

Koshnaw R.I., Horton B.K., Stockli D.F., Barber D.E., Tamar-Agha M.Y. & Kendall J.J. (2017) - Neogene shortening and exhumation of the Zagros fold-thrust belt and foreland basin in the Kurdistan region of northern Iraq. *Tectonophysics,* 694: 332-355.

Koshnaw R.I., Horton B.K., Stockli D.F., Barber D.E. & Tamar-Agha M.Y. (2020) - Sediment routing in the Zagros foreland basin: Drainage reorganization and a shift from axial to transverse sediment dispersal in the Kurdistan region of Iraq. *Basin Research*, 32(4): 688-715, 709.

Matsuoka A. (1984) - Late Jurassic four-segmented nassellarians (radiolaria) from Shikoku, Japan. *Journal of Geosciences, Osaka City University,* 27: 143-153.

Mazzullo J., Alexander A., Tieh T. & Menglin D. (1992) - The effects of wind transport on the shapes of quartz silt grains. *Journal of Sedimentary Research,* 62(6): 961-971, 970.

Müller J. (1858) - Über die Thalassicollen, Polycystinen und Acanthometren des Mittelmeeres. F. Dümmler.

O'Dogherty L. (1994) - Biochronology and paleontology of mid-Cretaceous radiolarians from northern Apennines (Italy) and Betic Cordillera (Spain). *Section des sciences de la terre, Université de Lausanne*, 1994, 413 pp.

Ozsvárt P., Bahramnejad E., Bagheri S. & Sharifi M. (2020) - New Albian (Cretaceous) radiolarian age constraints for the Dumak ophiolitic mélange from the Shuru area, Eastern Iran. *Cretaceous Research,* 111: 104451.

Parona C. (1890) - Radiolarie nei noduli selciosi del calcare giurese di Cittiglio presso Laverno. *Bollettino della Socieà Geologica Italiana*, 9: 132-175.

Pessagno E.A. (1976) - Radiolarian zonation and stratigraphy of the Upper Cretaceous portion of the Great Valley sequence, California Coast Ranges. *Micropaleontology, Spec. publ.,* 2: 1-95.

Pessagno E.A. (1977) - Lower Cretaceous radiolarian biostratigraphy of the Great Valley sequence and Franciscan complex, California coast ranges. Cushman Foundation for Foraminiferal Research, 1977, 87 pp.

Pessagno E.A., Six W.M. & Yang Q. (1989) - The Xiphostylidae Haeckel and Parvivaccidae, n. fam. (Radiolaria) from the North American Jurassic. *Micropaleontology*: 193-255.

Riedel W. (1967) - Some new families of Radiolaria. *Proceedings of the Geological Society of London*, 1640: 148-149.

Squinabol S. (1904) - Radiolarie cretacee degli Euganei. *Atti e Memorie della Reale Accademia di Scienze Lettere ed Arti in Padova*, Nuova Serie 20: 171-244.

Stoecklin J. (1968) - Structural history and tectonics of Iran: a review. *AAPG Bulletin,* 52(7): 1229-1258, 1230.

Takahashi K. & Honjo S. (1983) - Radiolarian skeletons: size, weight, sinking speed, and residence time in tropical pelagic oceans. Deep Sea Research Part A. *Oceanographic Research Papers,* 30(5): 543-568.

Vergés J., Sandra E., Casciello E., Fernandez M., Villaseñor A., Jimenez-Munt I. & García-Castellanos D. (2011) - Crustal-scale cross-sections across the NW Zagros belt: implications for the Arabian margin reconstruction. *Geological Magazine,* 148(5-6): 739-761.

Yang Q. (1993) - Taxonomic studies of Upper Jurassic (Tithonian) radiolaria from the Taman Formation, east-central Mexico. *Palaeoworld,* 3: 164.